

Investigation of Scale Inhibition Mechanism by Electrochemical Quartz Crystal Microbalance

Yuan Lu¹, Qiang Wei¹, Yan Cheng, Xiedong Ren², Hu Wang^{2,3,*}, Juan Xie^{2,*}

¹ CenerTech Oilfield Chemical Co., Ltd., CNOOC, Tianjin, 300450

² School of New Energy and Materials, Southwest Petroleum University, China, 610500

³ Research Centre of Corrosion and Protection for Materials in Oil and Natural Gas exploitation, Southwest Petroleum University, China, 610500

*E-mail: hwang@swpu.edu.cn (Hu Wang); jxie@swpu.edu.cn (Juan Xie)

Received: 26 November 2020 / Accepted: 21 January 2021 / Published: 31 March 2021

In this paper, electrochemical quartz crystal microbalance (EQCM) was applied to evaluate scaling and scale inhibitors by applying cathodic potential (potentiostatic polarization) on working electrode (quartz crystal microbalance wafer). The mass variation of scale deposited on wafer surface was in situ monitored by the EQCM. The scaling kinetic parameter and inhibition efficiency in the presence of scale inhibitor were obtained. Scaling in static and dynamic conditions of four tested scale inhibitors, POCA, HEDP, ATMP and SHMP, had been studied. All the inhibitors exhibited remarkable inhibition performance, with the inhibitor concentration ranging from 1 mg/L to 20 mg/L. Adding scale inhibitor during the scaling process displayed much better inhibition effect than adding it preferentially. Inhibition mechanism of four inhibitors is quite different, which can be revealed by combining accelerating scaling experiment, SEM and XRD.

Keywords: A1. Crystal morphology, A1. Nucleation, A2. Electrochemical growth, B1. Calcium compound, A3. Quartz crystal microbalance

1. INTRODUCTION

Calcium carbonate scale commonly occurs in many industrial applications, especially in oil or natural gas exploitation and industrial circulating cooling water [1-4]. The scaling usually leads to decrease in pipeline transmission capacity, which weakens the heat transfer efficiency and promotes the deposit corrosion. It is universally believed that the incompatibility of cation and anion in solution causes the scaling. The variations in temperature, flow condition or partial pressure of CO₂ in atmosphere have remarkable influence on scaling. Adding scale inhibitor is considered as one of the most useful measures to alleviate scaling. Many commercial scale inhibitors had been exploited and applied in application [5-

7]. Phosphonates are most commonly used in industry. However, prediction and evaluation of the effectiveness of the scale inhibitors with simple, accurate and fast method are still a great challenge [8-11].

Many existing laboratory tests had been developed to evaluate scaling and scale inhibitor [12-15]. However, most of the methods are mainly based on evaluating the precipitation rate in bulk solution, which is regarded, by some researcher, as no direct relation with scaling condition on solid surface [16-19]. Recently, an electrochemical technique based on quartz crystal microbalance (QCM) has been introduced into real-time monitoring scaling on solid surface. The real precipitation mass amount at solid can be measured with time. Therefore, the scaling kinetics and effectiveness of inhibitor can be measured. Additionally, the results by this method are very close to the real production condition.

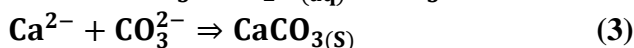
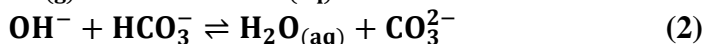
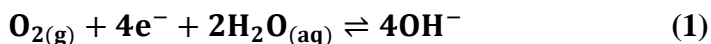
Some investigations have been carried out by EQCM (electrochemical quartz crystal microbalance). N. Kohler [16] presented EQCM for static and dynamic experiments for nucleation, growth and inhibition of CaCO_3 scaling. The scaling process had been recorded quantitatively and in situ microvision also incorporated to reveal the scaling process. Electrochemical, electrogravimetric and optical methods were applied to analyze the impact of magnesium ion on CaCO_3 scaling by O. Devos [19]. The concentration of Mg^{2+} has pronounced influence on scaling of nucleation, growth and crystal morphologies. N. Abdel-Aal [20] studied on the impact of a phosphonate inhibitor (EDTMP) on the scaling of CaCO_3 scale. It was studied by EQCM on solid surface and ion concentration measuring in bulk solution. The deposited CaCO_3 on QCM wafer surface and ion activity of the solution were monitored with time prolonged. The concentration of EDTMP on inhibition of scaling was also discussed. The inhibition of EDTMP to scaling can be ascribed to the adsorption of the scale inhibitor at the nuclei of scale. The presence of scale inhibitor induces deformation of the crystal morphology. L. Yua [21] applied quick evaluation of scale inhibitor by cathodic polarizations method. It was found that the antiscaling efficiency goes with order of $\text{PBTCA} \approx \text{HEDP} \gg \text{PAA}$. The presence of scale inhibitor in solution has critical impact on the type of scale crystal, from orthorhombic to hexagonal crystal. The different crystal structures imply the adsorption and inhibition on scale growth. However, more information on the inhibition mechanism regarding influence on crystal structures is still unclear. Further investigation is necessary in this field.

The present work concerns the accelerated scaling behavior in different scale inhibitors conditions. The scaling amounts on QCM wafer surface were recorded by EQCM with applying -1.4 V potential (vs. SCE). The inhibition efficiencies of scale inhibitors, POCA, HEDP, ATMP and SHMP were calculated and the inhibition mechanism of the inhibitors was also analyzed via SEM and XRD analysis.

2 EXPERIMENTAL DETAILS

Electrochemical quartz crystal microbalance (EQCM) was used for accelerating scaling [22-25]. The scheme of EQCM for accelerating scaling is shown in Fig. 1. QCM (QCM200, SRS, USA) was connected to electrochemical station (Iviumstat Electrochemical Interface, Ivium Technologies, Netherlands). Traditional three electrode measurements were applied, in which QCM wafer plated with

gold was used as the working electrode (WE), saturated calomel electrode (SCE) as reference electrode (RE) and platinum as counter electrode (CE). In accelerating scaling experiment, potentiostatic polarization method was applied with potential of -1.4 V (vs. SCE). Before potentiostatic polarization, open circuit potential (OCP) was monitored for more than 3 minutes to assure the relative stable of OCP. The electrochemical reaction and corresponding scaling process at cathodically polarized electrode are as follows:



The mass variation of scale deposited at QCM wafer can be recorded and calculated from the quartz crystal resonance frequency Δf by Sauerbrey equation:

$$\Delta f = -\frac{2f_0^2}{S(\mu\rho)^{1/2}} \cdot \Delta m \quad (4)$$

where Δf stands for the change of quartz crystal resonance frequency, f_0 is natural frequency of QCM wafer, S is the surface area of gold (wafer), ρ is the quartz density, μ is the shear modulus of quartz and Δm is mass variation. Mass variation during scaling can be monitored in real time.

The blank solution contains 200 mg/L Ca^{2+} , 610 mg/L HCO_3^- and NaCl for balance. All the scale inhibitors are commercial products produced in China (Shandong Taihe Water Treatment Technologies, Co., Ltd.), including copolymer of phosphono and carboxylic acid (POCA), 1-hydroxyethylidene-1,1-diphosphonic acid (HEDP), amino trimethylene phosphonic acid (ATMP) and sodium hexametaphosphate (SHMP). The temperature in all experiments was $50 \pm 0.1^\circ\text{C}$. In dynamic scaling experiment, the magnetic stirring was applied to obtain different stirring rate. Rotation speed of 10 r/s corresponds to linear velocity of 0.64 m/s. 20 r/s and 30 r/s equal to 1.28 m/s and 1.92 m/s, respectively.

Morphology observation was carried out after accelerating scaling experiment by SEM (EVO MA15, ZEISS). The crystal structure of scale was also characterized after accelerating scaling experiment using XRD (X' Pert MPD PRO, PANalytical B.V.).

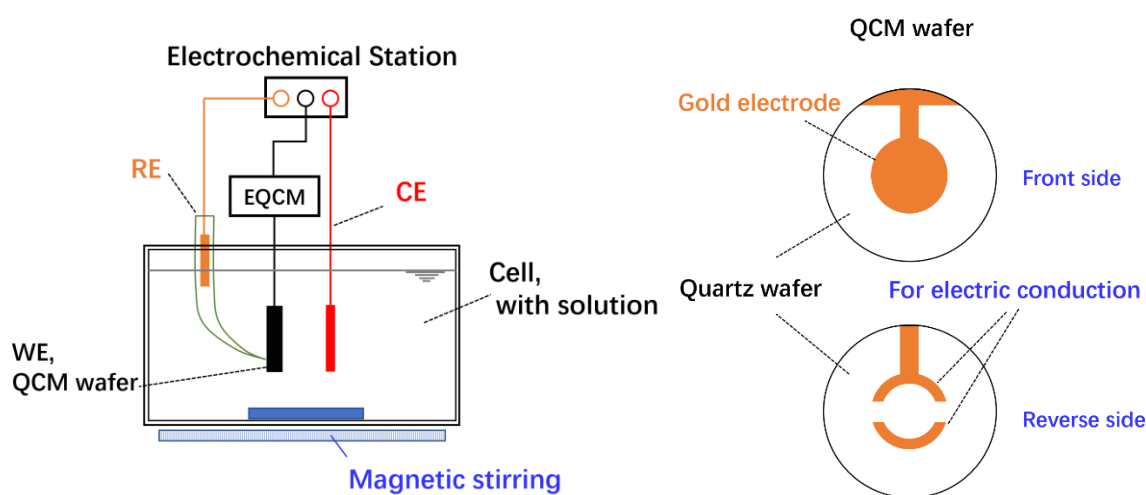


Figure 1. Schemes of EQCM for accelerating scaling (left) and QCM wafer (right).

3. RESULTS AND DISCUSSION

3.1 Influence of scale inhibitor on scaling.

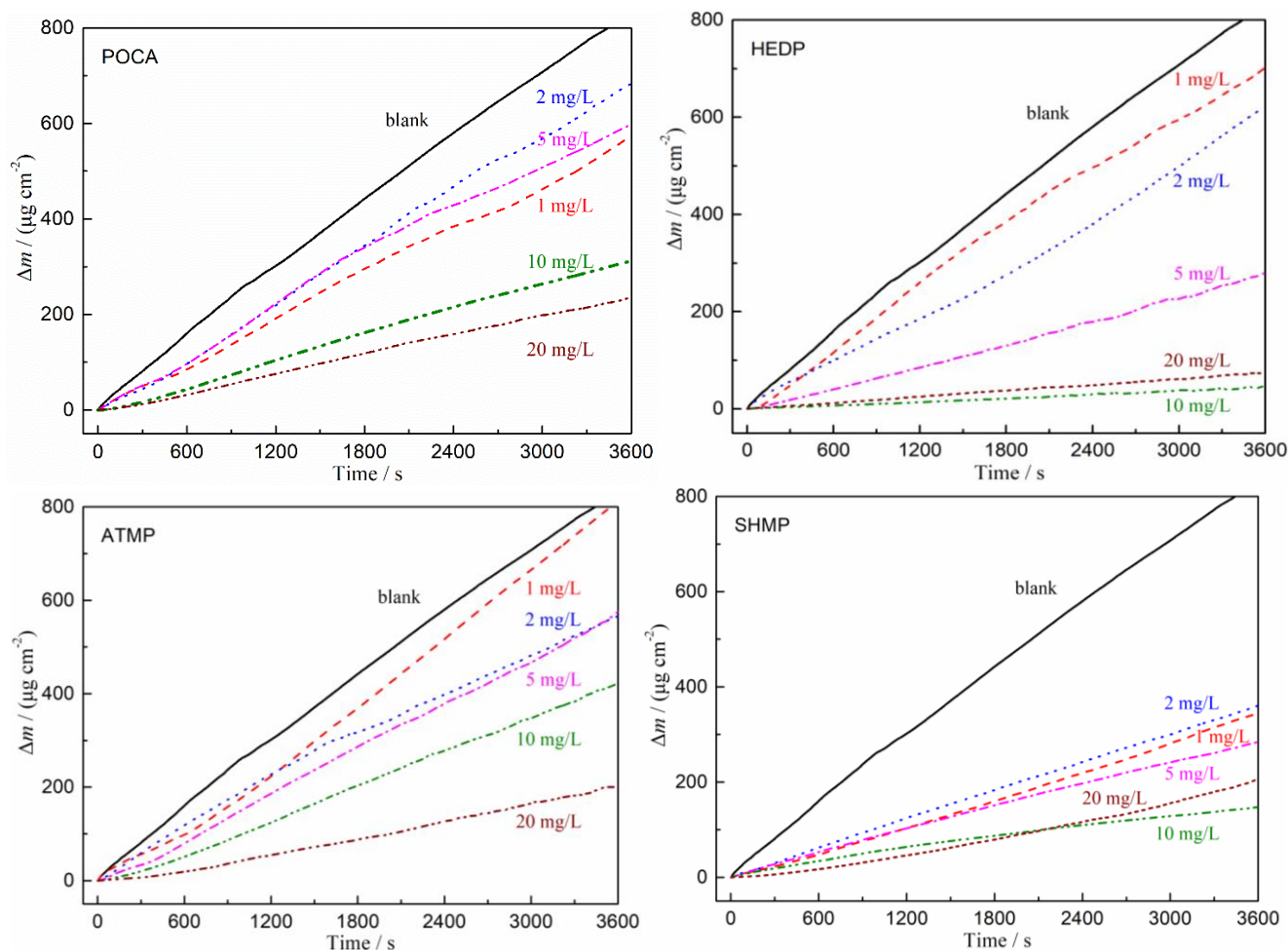


Figure 2. Scale inhibition from recording mass variations vs. time by EQCM in real time with inhibitors of POCA, HEDP, ATMP and SHMP at concentrations of 1 mg/L, 2 mg/L, 5 mg/L, 10 mg/L and 20 mg/L.

Fig. 2 shows the scaling amount variations with time in different types and concentrations of scale inhibitors. Four inhibitors, including POCA, HEDP, ATMP and SHMP, were used as scale inhibitors for the measurements with the concentrations of 1 mg/L, 2 mg/L, 5 mg/L, 10 mg/L and 20 mg/L, respectively. It is shown that all the three inhibitors exhibit obvious inhibition effects. With the increase of concentration, inhibition effects have been enhanced notably. It also can be seen in the figures that the increase of scaling amount with time obeys near linear behavior. Scale inhibitors like polycarboxylic acids inhibit scaling by coordinating the anionic functional groups to Ca^{2+} in solution or upon the CaCO_3 crystal surface [26,27]. Other scale inhibitors like polycarboxylic acids can also impede scaling by providing strong ability in chelating Ca^{2+} [28,29].

In order to quantitatively evaluate the scaling rate and inhibition effects by inhibitors, kinetic parameters were involved to elucidate it [30]. The scaling intensity can be directly recognized by the

slope of the curve. The steep curve, with big slope, implies the fast scaling rate. Hence, here we introduce a new definition to inhibition efficiency of scale inhibitor, which can be calculated as follows:

$$\eta = \frac{k_0 - k_1}{k_0} \times 100\% \tag{5}$$

where η is the inhibition efficiency, k_0 is the slope of fitted line without adding scale inhibitor (blank) and k_1 is derived from slope of the fitted line in the presence of scale inhibitor. Fitting of scaling curve is presented in Fig. 3 and corresponding data of parameters obtained from fitting are also displayed in Table 1.

k value in Table 2 reveals the growth kinetics of scale in different solution. In blank solution, without adding any scale inhibitor, k value is high up to $0.230 \mu\text{g}/(\text{cm}^2 \text{s})$, indicating that the scale grows with a high rate. In the presence of scale inhibitor, k value declines more or less, implying the effectiveness of the scale inhibitor. In most circumstances, k values decrease with the increase of inhibitor concentration. The smallest value of k occurs in HEDP 20 mg/L, which means the best inhibition effect on scaling. The behavior of inhibition efficiencies under different conditions also accords the same variations as kinetic parameter k , as can be seen in Table 1. Similar measurements had been used in previous studies [16,31]. However, the data analysis methods presented here had not been reported in previous studies.

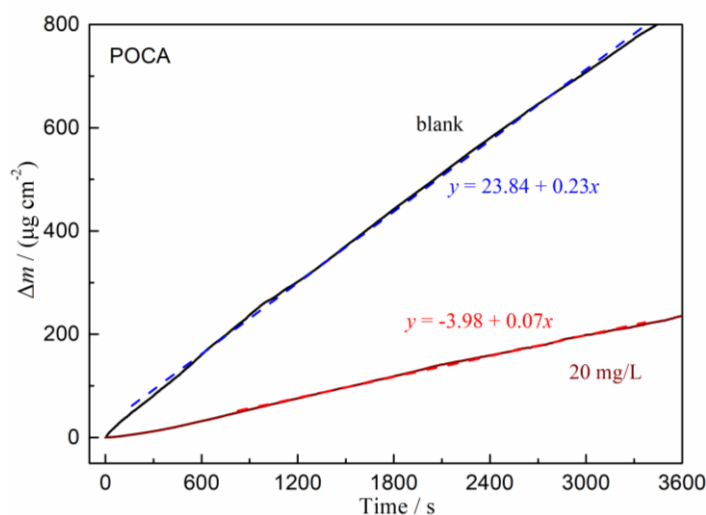


Figure 3. Examples of linear fitting of scale growth curve by POCA in the absence and presence of 20 mg/L.

Table 1. Inhibition efficiencies obtained from slope of scale growth curves in Figure 2 by fitting method of Figure 3.

inhibitor	concentration / (mg L ⁻¹)	k / (μg cm ⁻² s ⁻¹)	η / %
blank	0	0.230	-
POCA	1	0.155	32.6
	2	0.197	14.4
	5	0.164	28.7
	10	0.090	60.9

	20	0.070	69.6
HEDP	1	0.194	15.7
	2	0.171	25.7
	5	0.164	28.7
	10	0.013	94.4
	20	0.021	90.9
ATMP	1	0.235	-2.2
	2	0.150	34.8
	5	0.161	30.0
	10	0.124	46.1
	20	0.060	73.9
SHMP	1	0.098	57.4
	2	0.099	57.0
	5	0.078	66.1
	10	0.037	83.9
	20	0.060	73.9

3.2 The inhibition effects in adding scale inhibitor at scaling process.

In order to understand the diffusion of scale inhibitor on inhibition effects, adding scale inhibitor during scaling process had been applied. This method is more close to industrial application of scale inhibitor. The experiments can be illustrated as Fig. 4 (left). The scaling process can be classified into three stages. The first stage is the accelerating scaling in blank solution. Then it proceeds into the second stage, transition stage, in which 5 mg/L POCA is added into the solution after scaling in blank solution for about 1000 seconds.

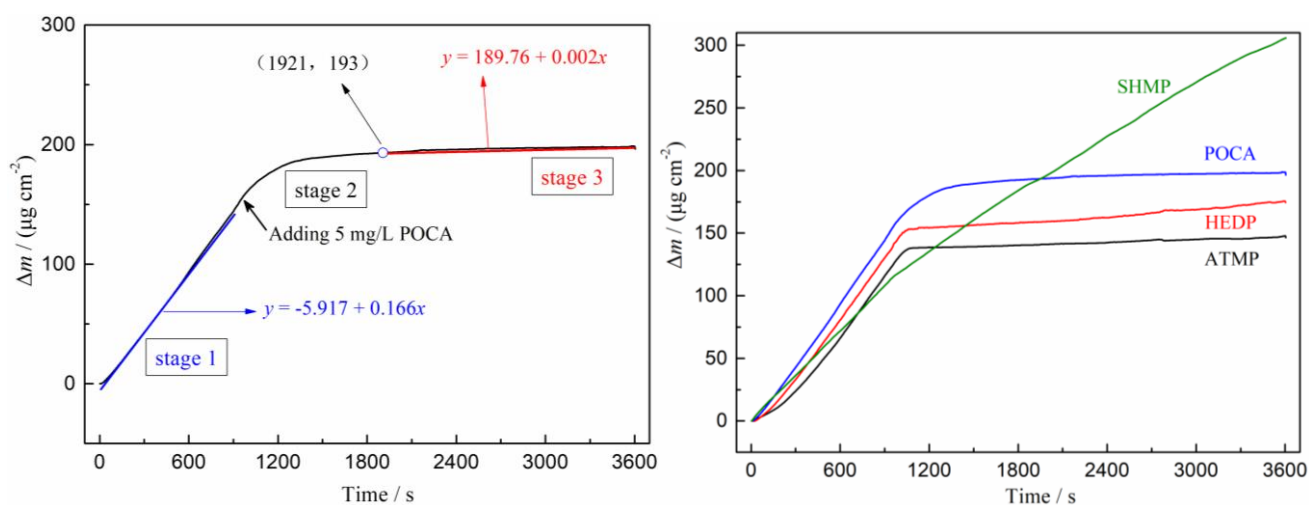


Figure 4. Adding scale inhibitor during scaling process, example of fitting (left), scaling experiments by adding different inhibitor, POCA, HEDP, ATMP and SHMP, with the concentration of 5 mg/L during scaling process by EQCM (right).

The diffusion and inhibition effects of POCA molecules gradually undergo. The stable state of scale growth is slowly reached and stage 3 comes into being. In stage 3, the scaling process is inhibited to some extent, which depends on the effectiveness of scale inhibitor, the type and concentration of it. The growth kinetic parameter k in stage 1 and stage 3 can be obtained by fitting the scale growth curve at two different stages, respectively. The inhibition efficiency of inhibitor can also obtain by using similar method as equation (1).

The inhibition efficiency obtained by this method is more liable than using different curves of different scaling experiments. The effectiveness of scale inhibitor can be directly presented, as shown in Fig. 4 (right). In Fig. 4 (right), it is evidently that 5 mg/L POCA, HEDP, ATMP are very effective in inhibiting scaling. Additionally, the k values of stage 3 of the three inhibitors are apparently smaller than the ones obtained in Fig. 2. It demonstrates that the inhibitor is more effective to inhibit scaling at the surface of existed scale. However, SHMP is almost useless, which is quite different from the result in Fig. 2. SHMP is an inorganic phosphate, which is commonly not very stable and sometimes hard to dissolve and diffuse in solution. If it has been keeping standing for a period, the SHMP molecules will hydrolyze. In neutral or alkaline solution, it would possibly react with Ca^{2+} to form scale. Additionally, the bad effectiveness of SHMP can also be attributed to inhibition mechanism, by the chelation of Ca^{2+} in bulk solution, not by adsorption on existed scale.

3.3 The influence of flow rate on inhibition effects.

Flow rate of solution is an important factor to influence the scaling process. S. Sutomo proved mass scale would be promoted at higher flow rate [32]. Additionally, the flow rate influences the formation of scales too and makes the crystal type transformed from vaterite to calcite and aragonite. The influence of flow rate on inhibition effects has been investigated with adding different scale inhibitors of 5 mg/L during the intermediate process of scaling. Fig. 5 displays the scaling behaviors of POCA, HEDP, ATMP and SHMP at flow rate of 30 r/s, 20 r/s, 10 r/s and static condition, respectively. It shows that flow rate has remarkable influence on scaling process. At the first stage of scaling, before adding scale inhibitor, the elevating of flow rate is beneficiary to scaling. The faster the flow rate, the higher the scaling rate will be. The kinetic parameter, k_1 , reveals the variation behavior at different flow rate, as shown in Table 2. However, in 10 r/s of POCA, the k_1 is less than static condition. Additionally, all the k_1 at the same flow rate should be the same. The results shown in Table 2 demonstrates quite different values. The reason can be ascribed to error caused by different surface condition of the gold electrode. Therefore, comparison between k_1 and k_3 in the same curve is more accurate. k_3 , presented in Table 2, shows very small values in most conditions except SHMP, which indicates the scaling process has been well inhibited in most conditions. Additionally, the inhibition effects are stronger than adding inhibitor preferentially. This behavior can be easily recognized by comparing k in Table 1 and k_3 in Table 2. The better inhibition effects can be explained by flowing condition of the solution. With the adding of scale inhibitor at flow condition, the inhibitor can be fast dissolved and diffused. The inhibitor molecules will be dispersed in solution and inhibition effects will be enhanced promptly. Inorganic inhibitor SHMP exhibits bad effects in static and dynamic (20 r/s) conditions. More experiments of flow

rates are unnecessary. The inhibition effectiveness of SHMP is more complex than organic inhibitors. The pre-dissolving, standing and hydrolyzing processes have very crucial influence on SHMP. In application, inorganic inhibitors like SHMP are unstable in performance and bad to environment. It has already been eliminated.

Nucleation time (t_N) [16] can be obtained for different conditions, which is fitted from the slope of the original linear curve of the $\Delta m-t$ plot, corresponding to the nucleation of crystal seeds or the inhibition started of crystal and the crystal growth initiation. It reveals in Table 2 that in static condition or lower flow rate (10 r/s and 20 r/s), t_N keeps at a relative big value. While in 30 r/s, t_N remarkably drops to a rather low value. The results indicate that the nucleation of scale has been greatly shortened in 30 r/s. The enhancement of diffusion of Ca^{2+} and CO_3^{2-} by higher flow rate accelerated the scaling nucleation process. Moreover, with the increase of ions diffusion at interface, the scaling amount notably increases with flow rate.

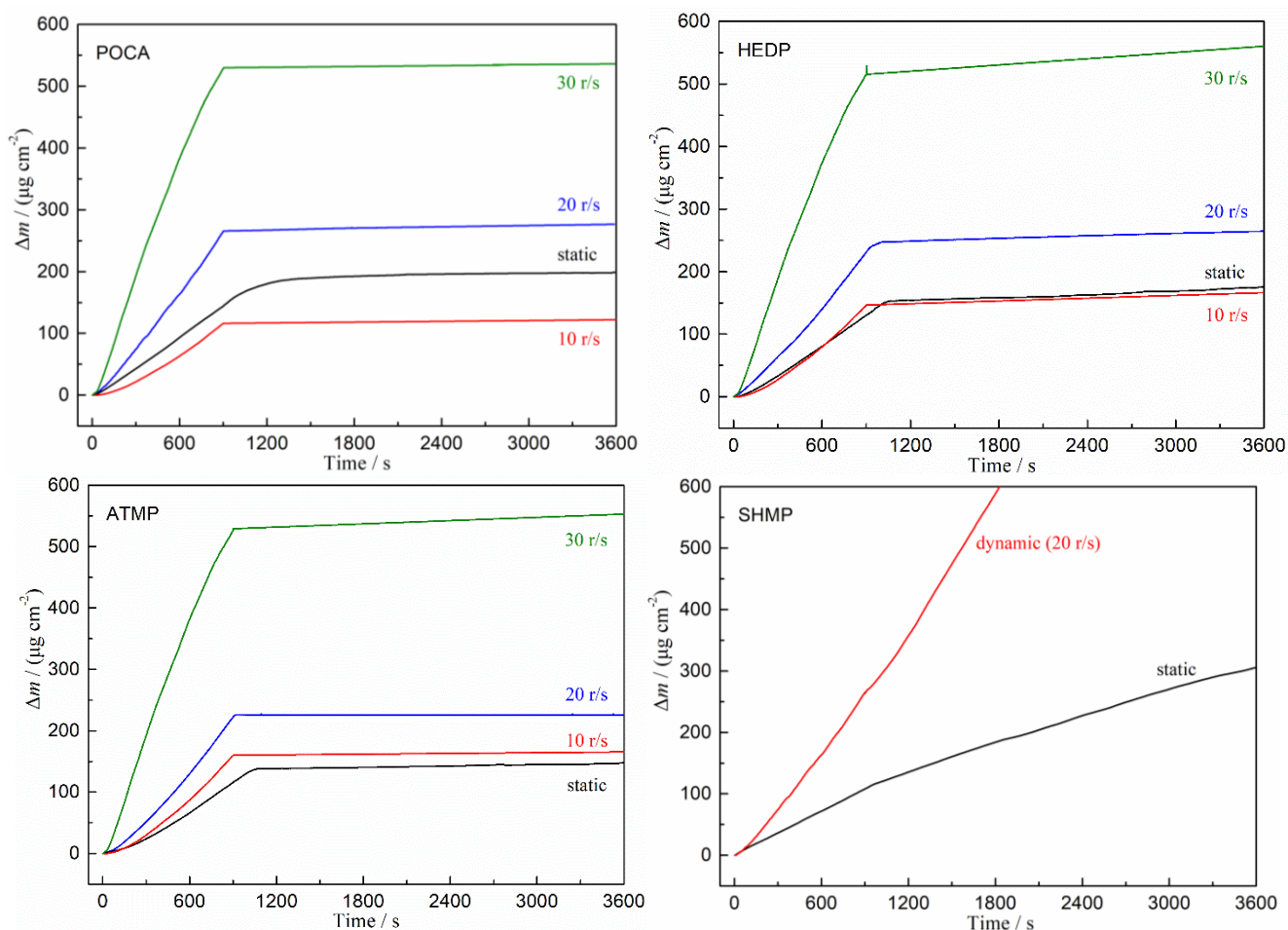


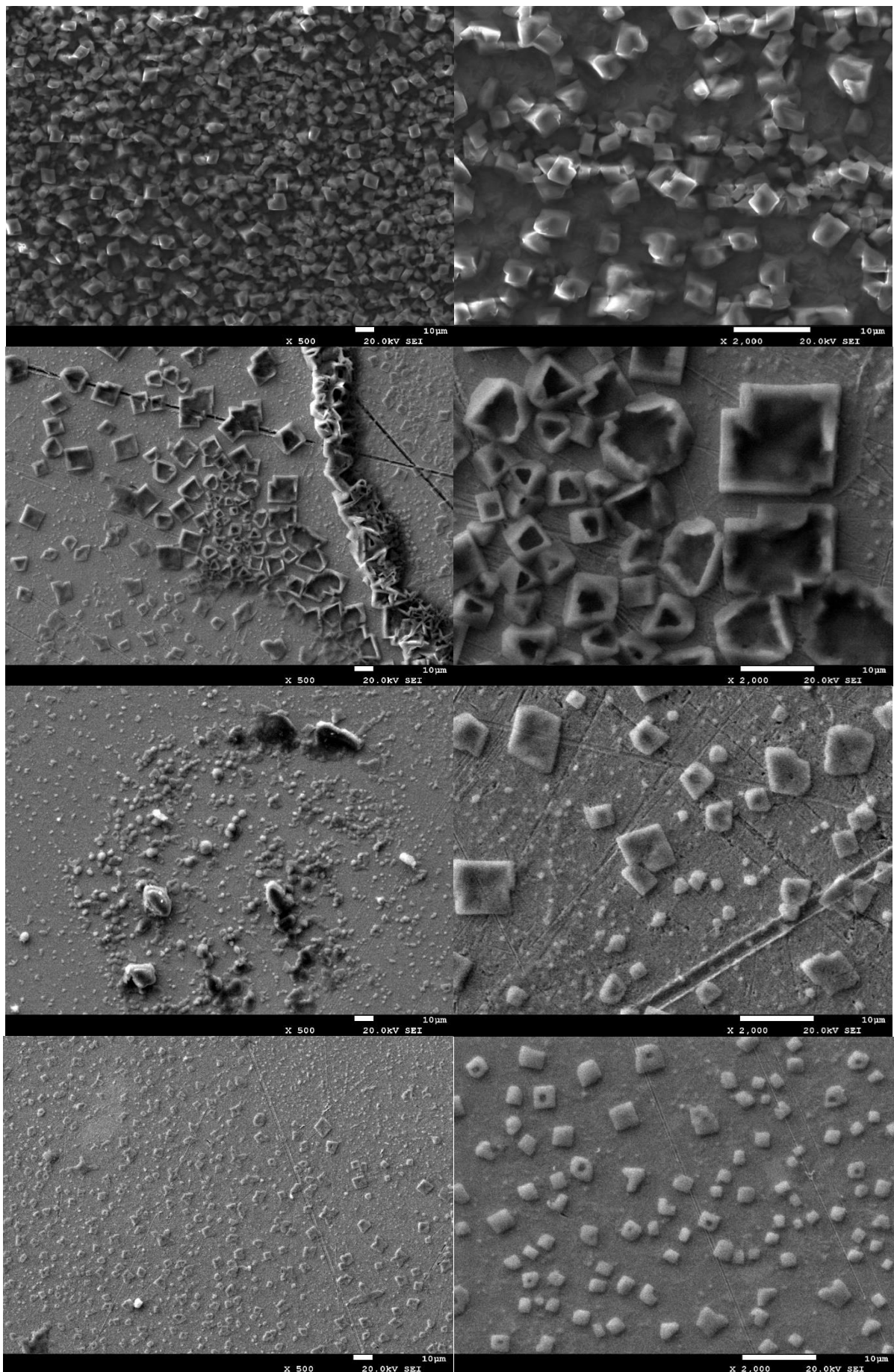
Figure 5. Influence of flow rate on scaling in the presence of different scale inhibitors, POCA, HEDP, ATMP and SHMP, with the concentration of 5 mg/L by EQCM accelerating scaling technique.

Table 2. Scaling kinetic parameters and inhibition efficiencies at different flow conditions with different inhibitor dosages.

Inhibitor	flow condition	t_N / s	$k_1 / (\mu\text{g cm}^{-2} \text{s}^{-1})$	$k_3 / (\mu\text{g cm}^{-2} \text{s}^{-1})$	$\eta / \%$
POCA	static	35.72	0.166	0.002	98.5
	10 r/s	75.21	0.136	0.002	98.8
	20 r/s	45.31	0.300	0.005	98.4
	30 r/s	0.41	0.622	0.002	99.6
HEDP	static	67.06	0.153	0.009	93.4
	10 r/s	112.03	0.171	0.007	95.7
	20 r/s	47.60	0.260	0.007	97.4
	30 r/s	1.10	0.608	0.017	97.3
ATMP	static	91.97	0.135	0.004	97.3
	10 r/s	85.27	0.187	0.002	98.9
	20 r/s	78.19	0.256	0.001	99.8
SHMP	30 r/s	0.28	0.618	0.009	98.6
	static	-	0.118	0.071	39.8
	20 r/s	-	0.299	0.261	12.7

3.4 Inhibition mechanism of scale inhibitor.

The surface morphology after scaling for 1 hour can be observed by SEM [31]. Fig. 6 shows the surface morphologies of wafers after scaling in blank solution, 5 mg/L POCA, 5 mg/L HEDP, 5 mg/L ATMP, and 5 mg/L SHMP, respectively. The wafers used in SEM observation are from the measurements in 3.1. The magnification times for every condition are 500 \times and 2000 \times . SEM results demonstrate that the calcium carbonate scale piles up together with great amount in blank. The scaling is severe and the shape of the scale is cube. The distribution of the scale crystals is quite uniform. After adding any of the inhibitors, with 5 mg/L, the scaling extent weakens significantly. The adding of scale inhibitor tends to change the crystal structure and morphology of scale [26]. The single crystal of scale extends in size in POCA, ATMP and SHMP. In POCA, the distribution of scale crystals is not uniform. Scale crystals tend to propagate and pile together at some specific zones. The crystal size is also not uniform. It implies that the nucleation of scale preferentially occurs at active sites. The inhomogeneity at wafer surface is the main reason of nucleation. Such phenomenon is more apparent in HEDP, in which the nonuniform in distribution and crystal size are severe. In ATMP, the scale crystals distribute at wafer surface with uniform appearance. The sizes of crystals are not very even but all in relatively small sizes. Moreover, the shape of the crystals is not quite regular, which is different from other conditions. In SHMP, the number of crystals is not as many as in blank. However, the individual scale has been propagated to a rather large size. The shape of crystal is very regular cube.



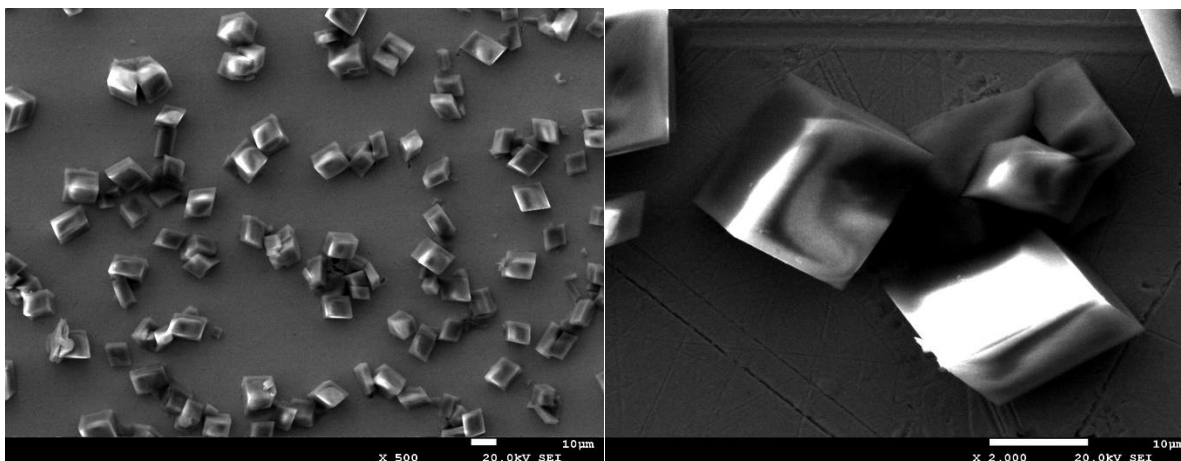


Figure 6. Morphologies of scale by SEM after accelerated scaling for 1 hour in: (a) and (b) blank; (c) and (d) 5 mg/L POCA; (e) and (f) 5 mg/L HEDP; (g) and (h) 5 mg/L ATMP; (i) and (j) 5 mg/L SHMP.

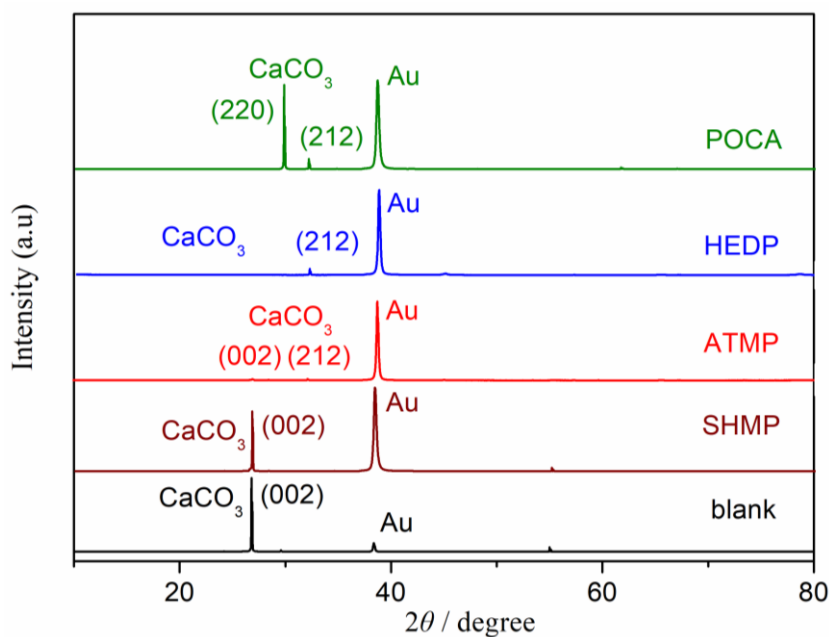


Figure 7. XRD patterns of scale crystals on QCM wafers in the absence and presence (5 mg/L different inhibitors) of different scale inhibitors after accelerating scaling experiments by EQCM.

Additional scale growth mechanism can be obtained by XRD analysis [21]. Fig. 7 is the comparison of XRD patterns of scales after accelerated scaling experiments at different conditions. The spectrum reveals all the scales are CaCO₃ crystals. Previous SEM observation can directly prove the variation of size of scale crystal in different inhibitor additions. More accurate variation of crystal size can be obtained from XRD by using Scherrer formula, which has been presented in equation (6).

$$D = \frac{K_{\gamma}}{B \cos \theta} \quad (6)$$

where D represents the average grain size, nm; K stands for Scherrer constant and $K=0.89$; γ is the wavelength of X-ray, $\gamma=0.154056$ nm; B is full width at half maximum (FWHM) and θ is diffraction angle, degree. The calculated results are shown in Table 3. The size order from large to small is: blank, SHMP, POCA, HEDP and ATMP. Therefore, the ability of inhibiting crystal growth is in the reversed order: ATMP, HEDP, POCA and SHMP.

Table 3. Average sizes of crystals (obtained from Fig. 6) calculated from XRD patterns by Scherrer formula.

Scale inhibitor	$B(\text{FWHM})$	D (nm)
blank	0.107	75.47
POCA	0.119	68.28
HEDP	0.242	33.74
ATMP	0.248	32.56
SHMP	0.107	75.46

Fig. 7 shows that the scale in blank solution displays strong intensity of CaCO_3 peak of (002), which implies the scale crystal grows mainly along (002) crystal face. The peak of Au is a good reference to compare the crystallinity of scales. The intensity ratio of peaks in XRD of CaCO_3 and Au is about 8.46, implying severe scaling at wafer surface.

In solution with 5 mg/L POCA, the XRD pattern behaves strong peak at (220) and weak peak at (212), not at (002) anymore. The peak intensity ratio of CaCO_3 (220) and (212) is 8.29, which proves that the scale propagates along (220) and (212) crystal faces, with (220) prevailing. Peak ratio of CaCO_3 (220) and Au is about 0.95. The grain size decreases from 75.47 nm in blank solution to 68.28 nm in 5 mg/L POCA. The scaling is inhibited regarding blank solution.

As for HEDP, the prevailing face is (212). The peak ratio of CaCO_3 (212) and Au is only 0.072, which means the weak crystallinity or weakness in scaling. The average grain size decreases to only 33.74 nm, implying the excellent inhibition effect.

The average grain size decreases to only 32.56 nm in the presence of 5 mg/L ATMP. It exhibits excellent performance in inhibiting scale crystalizing. The peaks in XRD appear at both (002) and (212). The both peaks are weak by comparing with Au. The peak intensity ratio between CaCO_3 (002) and Au is 0.015, and the one between CaCO_3 (212) and Au is 0.019. It shows that the crystallinity of CaCO_3 is very weak to Au and implies excellent inhibition effectiveness of ATMP. The peak intensity ratio of CaCO_3 (002) and (212) is 0.8, which means the growth in the two crystal faces are very close.

In SHMP, scale grows along (002), similar to blank solution, with moderate intensity. The peak intensity ratio between CaCO_3 (002) and Au is 0.72, which is much lower than 8.46 of blank solution. The grain size of 75.46 nm, very close to 75.47 nm of blank solution, suggests that the inhibition effect of SHMP to scale growth in crystal is very limited.

Different from peak at (002), the peaks of scales in POCA and HEDP occur at (220) and (212). It indicates that the inhibition mechanism is adsorption in nature, chelation and lattice distortion may

also have minor influence. In ATMP, the peak emerges at both (002) and (212). It means that the original scaling pattern has been partly inhibited and adsorption effect exerts an influence. In SHMP, the peak occurs at (002). The scale growth mechanism is similar with the absence of scale inhibitor (blank). The possible inhibition mechanism for SHMP is chelation of Ca^{2+} in bulk solution. The inhibition effect upon scale crystal is limited. Similar XRD patterns [6] revealed that the scale inhibitors impeded the scale propagation and reduced the surface coverage of CaCO_3 at interface. The presence of scale inhibitor PBTCA made the crystal type transform from original aragonite into unstable vaterite. S. Sutomo [32] also found that the increase of the flow rate enhanced the crystal type transformation from vaterite to calcite and aragonite. The adsorption of scale inhibitor at certain crystal face hampered the scaling process, like the influence of fluids with different flow rate.

4. CONCLUSIONS

Accelerating scaling technique by applying cathodic potentiostatic polarization is very effective in both evaluating effectiveness of scale inhibitor and in revealing antiscaling mechanism, by combining with SEM and XRD. The scale deposited on wafer surface was in situ monitored by the EQCM technique. The scaling kinetic parameter and inhibition efficiency with scale inhibitor were obtained. In static scaling study, four tested scale inhibitors, including POCA, HEDP, ATMP and SHMP, exhibited remarkable inhibition performance, with the inhibitor concentration ranging from 1 mg/L to 20 mg/L. Inhibition efficiency of any scale inhibitor basically rose with the rise of concentration. HEDP performed the best in inhibition efficiency in the four tested inhibitors. Adding scale inhibitor during the scaling process displayed much better inhibition effect, which is closer to the real application in industry. POCA, HEDP and ATMP had inhibition efficiencies more than 95%, which indicates the adsorption and lattice distortion effects on scale are the main reason of scale inhibition. Dynamic scaling experiment showed that flow rate had pronounced effect on scaling. Increasing flow rate is beneficial to ion diffusion at interface, which enhanced the scaling rate. Inorganic inhibitor SHMP behaved badly in antiscaling when added during the process of scaling, implying SHMP took into effect only by chelation of Ca^{2+} in solution. The scale deposited at different conditions had been characterized by SEM and XRD. Morphology observation showed very different in scale size, shape and distribution. XRD reveals different inhibition mechanism of the four inhibitors. The inhibition mechanism of POCA and HEDP is adsorption in nature, chelation and lattice distortion may also have minor influence. ATMP takes effect by adsorption effect and SHMP by chelation only.

ACKNOWLEDGEMENTS

This work was supported by Sichuan Key Lab of Oilfield Materials [Grant No. X151519KCL07].

References

1. J. Ma, C. Li, F. Liu, Y. Wang, X. Feng, *J. Clean. Prod.*, 199 (2018) 916.
2. M. Chaussemier, E. Pourmohtasham, D. Gelus, N. Pécoul, H. Perrot, J. Lédion, H. Cheap-

- Charpentier, O. Horner, *Constr. Build. Mater.*, 236 (2020) e117613.
3. A. Al Helal, A. Soames, S. Iglauer, R. Gubner, A. Barifcani, *J. Petrol. Sci. Eng.*, 173(2019)158.
 4. A. Quddus, L.M. Al-Hadhrani, *Desalination*, 246(2009)526.
 5. R. Menzri, S. Ghizellaoui, M. Tlili, *Desalination*, 404 (2017)147.
 6. Z. Zuo, W. Yang, K. Zhang, Y. Chen, M. Li, Y. Zuo, X. Yin, Y. Liu, *J. Colloid Interf. Sci.*, 562(2020)558.
 7. A. Neville, A.P. Morizot, *Chem. Eng. Sci.*, 55 (2000)4737.
 8. O.S. Sanni, O. Bukuaghangin, T.V.J. Charpentier, A. Neville, *J. Petrol. Sci. Eng.*, 182(2019) e106347.
 9. C. Gabrielli, M. Keddam, A. Khalil, R. Rosset, M. Zidoune, *Electrochim. Acta*, 42 (1997) 1207.
 10. C. Deslouis, C. Gabrielli, M. Keddam, A. Khalil, R. Rosset, B. Tribollet, M. Zidoune, *Electrochim. Acta*, 42 (1997)1219.
 11. M.F.B. Sousa, C.A. Bertran, *J. Colloid Interf. Sci.*, 420(2014)57.
 12. C. Gabrielli, M. Keddam, H. Perrot, *J. Appl. Electrochem.*, 26(1996)1125.
 13. A. Al Helal, A. Soames, S. Iglauer, R. Gubner, A. Barifcani, *J. Petrol. Sci. Eng.*, 179(2019)1063.
 14. Y. Zhao, Z. Xu, B. Wang, J. He, *Int. J. Heat Mass Tran.*, 141 (2019)457.
 15. T. Lourteau, H. Berriche, K. Kécili, V. Heim, H. Cheap-Charpentier, *J. Cryst. Growth*, 524 (2019)125161.
 16. N. Kohler, G. Courbin, F. Ropital, *SPE* 68963 (2001).
 17. R.G.M. de A. Macedo, N. do N. Marques, L.C. S. Paulucci, J.V.M. Cunha, R. de C. Balaban, *Carbohydr. Polym.*, 215(2019)137.
 18. P. Zhang, Y. Liu, N. Zhang, W.F. Ip, A.T. Kan, M.B. Tomson, *J. Ind. Eng. Chem.*, 702(2019)462.
 19. O. Devos, S. Jakab, C. Gabrielli, S. Joiret, B. Tribollet, S. Picart, *J. Cryst. Growth*, 311(2009)4334.
 20. N. Abdel-Aal, K. Sawada, *J. Cryst. Growth*, 256 (2003) 188.
 21. L. Yu, L. Liang, S. Liu, Y. Lv, J. Lin, H. Li, *Chem. Eng. Res. Des.*, 89(2011)1056.
 22. A. Morizot, A. Neville, T. Hodgkiess, *J. Cryst. Growth*, 198/199(1999)738.
 23. C. Garcia, G. Courbin, F. Ropital, C. Fiaud, *Electrochim. Acta*, 46 (2001) 973.
 24. C. Gabrielli, G. Maurin, G. Poindessous, R. Rosset, *J. Cryst. Growth*, 200 (1999) 236.
 25. A.P. Morizot, A. Neville, *SPE* 60189 (2000).
 26. A. Spinthaki, M. Kamaratou, G. Skordalou, G. Petratos, A. Tramaux, G. David, K.D. Demadis, *Geothermics*, 89 (2021) 101972.
 27. R.M. Haaring, N. Kumar, D. Bosma, L. Poltorak, E. J. Sudholter, *Energ. Fuel.*, 33(2019)805.
 28. X.C. Li, B.Y. Gao, Q.Y. Yue, D.F. Ma, H.Y. Rong, P. Zhao, P.Y. Teng, *J. Environ. Sci.*, 29 (2015) 124–130.
 29. K.S. Song, J. Lim, S. Yun, D. Kim, Y. Kim, *Int. J. Heat Mass Transf.*, 136(2019) 555.
 30. K. Harouaka, A.T. Kan, M. Tomson, *Appl. Geochem.*, 109 (2019)e104393.
 31. K.S. Raj, N. Devi, V.K. Subramanian, *Chem. Phys. Lett.*, 750(2020)e137502.
 32. S. Sutomo, S. Muryanto, W. Mangestiono, J. Jamari, A. P. Bayuseno, *Mater. Today Proc.*, 13 (2019) 287.